Evidence of 1D Behavior of He^4 Confined within Carbon-Nanotube Bundles

J. C. Lasjaunias,[1] K. Biljaković,[2] J. L. Sauvajol,[3] and P. Monceau[1,4]

[1]*Centre de Recherches sur les Très Basses Températures, CNRS, BP 166, 38042 Grenoble Cedex 9, France*
[2]*Institute of Physics, Hr-10 001 Zagreb, P.O.B. 304, Croatia*
[3]*Groupe de Dynamique des Phases Condensées, Université Montpellier II, 34095 Montpellier Cedex 5, France*
[4]*Laboratoire Leon Brillouin, CEA-CNRS, CEA Saclay 91191 Gif-sur-Yvette Cedex, France*

(Received 22 January 2003; published 11 July 2003)

We present the first low-temperature thermodynamic investigation of the controlled physisorption of He^4 gas in carbon single-wall nanotube (SWNT) samples. The vibrational specific heat measured between 100 mK and 6 K demonstrates an extreme sensitivity to outgassing conditions. For bundles with a few number of nanotubes the extra contribution to the specific heat, C_{ads}, originating from adsorbed He^4 at very low density displays 1D behavior, typical for He atoms localized within linear channels as grooves and interstitials, for the first time evidenced. For larger bundles, C_{ads} recovers the 2D behavior akin to the case of He^4 films on planar substrates (grafoil).

DOI: 10.1103/PhysRevLett.91.025901 PACS numbers: 65.80.+n, 68.43.–h, 68.65.–k

The discovery of carbon nanotubes is very exciting from the academic point of view, but also for engineering purposes. Reducing dimensionality can bring entirely new properties for the thermodynamics of vibrational states for nanotubes as well as for the mechanisms of gas adsorption (in structures such as bundles), in particular He^4, which has already been largely investigated in the 2D case. 1D confinement of vibrational modes was supposed to explain the specific heat (C_p) in single-wall nanotubes (SWNTs) measured down to 2 K [1]. He within the interstitials in nanotube bundles was expected to condense into a lattice gas [2]. Our recent C_p measurements did not support these both expectations [3]; but they yielded C_p results of pristine nanotubes and showed a remarkable influence of a relatively small quantity of adsorbed He, which, in particular, allows the comparison to the case of He films in 2D configurations, already largely investigated [4–6].

In this Letter we present the low-temperature (T) specific heat investigation on two SWNT samples in similar conditions as far as adsorbed He^4 is concerned. The first sample was prepared by laser vaporization (sample LV) and the second one by electric-arc discharge (sample AD). X-ray and neutron diffraction and Raman experiments were used for the characterization of both samples [7,8].

Sample LV (synthesized in "Rice University conditions" [9]) was obtained by laser vaporization at 1100 °C with Ni and Co catalysts, up to 2 at.% as residual concentration in final samples. The SWNTs of mean diameter 1.4 nm, with a standard deviation of 0.2 nm [8], form bundles organized in the usual hexagonal lattice of parameter 1.7 nm. Bundles with a diameter of 10–13 nm contain typically 30–50 tubes, with an extension up to 20 nm (i.e., up to $N_t \sim 100$ tubes). The LV sample ($m = 45$ mg) in the form of several elastic foils (buckypaper as in Ref. [1]) was used for previous heat capacity measurement [3]. *Sample AD* was synthesized at Montpellier by arc discharge [10] with Ni (0.5%) and Y catalysts (0.5%), in total 1 at.%, and with no Co. The individual SWNTs of similar diameter as in sample LV [7,8] here are organized in bundles generally smaller in diameter — up to 10 nm with N_t less than 20–30 tubes. The AD sample ($m = 90$ mg) was in a form of pellet (13 mm in diameter, 1 mm thick) obtained by pressurization of powder with 10 kbar [11]. Within the usual purification technique, the nanotubes are close ended. So, we suppose that no adsorption can occur within the tubes, and only interstitials or external grooves and surfaces of the bundles are the most probable occupancy sites. Both samples were mounted in the same manner [3] in a glove box under nitrogen atmosphere to avoid at maximum gaseous contamination from ambient air and thereafter transferred in the dilution cryostat. The data were collected by the transient heat pulse method between 100 mK and 6 K.

We have studied the adsorption in LV and AD samples by simply using our usual cooling procedure down to 4.2 K, He^4 being the exchange gas [3]. After initial pumping at room temperature, He^4 is introduced in the calorimeter chamber at 77 K at a pressure of $(6–7) \times 10^{-2}$ mbar. Normally, when the sample does not adsorb, at 4.2 K we pump out the exchange gas in order to get good conditions for C_p measurements ($\sim 10^{-6}$ mbar). Spectacularly, in LV samples all the He^4 was adsorbed, so that cooling down to He temperature was not possible without a new injection. This was the first evidence of the strong He adsorption in SWNT samples. As it is well established that He^4 is totally desorbed by reheating up to 25–30 K [1,3,12], we used this procedure to obtain the first desorbed state (as for run A in Ref. [3]). In addition, a further long secondary pumping (a few days to a whole week) at 300 K, coupled with the above very efficient desorbing procedure (reheating from 4.2 to 40 K) was

used to define the heat capacity in the best outgassing conditions (run C for the LV sample [3] and III in the AD sample).

Figure 1 presents the new data collected on the AD sample. State I was obtained with the usual He dose for cooling the sample down to 4.2 K and successive pumping under secondary vacuum at 5 K. State II corresponds to more efficient outgassing conditions — reheating under active pumping up to 15 K. As this temperature is too low for a complete desorption, this run represents a case of intermediate He adsorption. The most efficient desorption procedure was performed for state III. First the sample was under active secondary pumping during one week at 300 K. Afterwards it was cooled down to 4.2 K (following procedure I). Finally, further reheating to 35–40 K enabled complete outgassing of He. Consequently, we take C_p of state III as the *pristine* nanotube value, corresponding to the vibrational contribution. Here we indicate only that the extrinsic contribution of the ferromagnetic catalyst (identical for I, II, and III, similarly as in Fig. 1 in Ref. [3]), which shows up via a nuclear hyperfine term C_N (rising below 0.15 K), was much smaller than in the LV sample due to the absence of Co [13]. This term is subtracted and the vibrational heat capacity $C_{\text{vib}} = C_p - C_N$ is reported for the three runs in Fig. 1. There is an evident and progressive decrease of C_p on improving the outgassing. In comparison to the pristine data (state III), adsorption of He results in a broad anomaly for state II entirely included in our investigated T range. This was also the case in the LV sample (run A compared to C in Ref. [3]).

Another contribution becomes predominant below 0.5 K, which is *not related* to He adsorption, as it is almost the same for both states II and III [14]. It exists also in the LV sample and it can be represented by a sublinear power law $\sim T^{\alpha}$, with $\alpha = 0.34$ in AD and $\alpha = 0.62$ in LV, usually ascribed to localized low energy excitations (defects in the carbon lattice and/or the nanotube itself [15]). Finally, C_{vib} in the pristine state (III) of the AD sample is the sum of two terms for $T \leq 1.8$ K: $C_{\text{vib}} = A\,T^{\alpha} + \beta\,T^3 = 0.061\,T^{0.34} + 0.072\,T^3$ (mJ/g K). The second term represents the Debye phononic contribution, which indicates the 3D character of the bundles for low-frequency phonon modes. The cubic regime is no more obeyed above 1.8 K, where C_{vib} changes smoothly to a quadratic regime. The lower crossover temperature T_{co} in AD indicates that the transversal lattice cohesion is weakened compared to LV [3], which is consistent with a smaller number of tubes N_t in the bundle. This softening of the intertube cohesive forces — decrease of transverse sound velocity — is also in agreement with the larger β, being 0.072 mJ/g K^4 in AD compared to 0.035 mJ/g K^4 in LV [3,15].

To go further with the analysis, we make the assumption that the contribution of adatoms to the specific heat is additional to that of the pristine SWNT. It holds to a great accuracy due to the fact that the adsorbate modes couple only weakly to the substrate vibrational modes (the substrate atomic mass mismatch is large —4/12). Hence we obtain C_{ads} after subtracting the corresponding pristine values; run C for LV [3] and state III for AD. C_{ads} for the maximum adsorption is presented in Fig. 2 and for the case of intermediate adsorption in Fig. 3. Here we repeat that the pressure of He^4 gas admitted in the sample chamber was the same in both cases (corresponding to $N_0 = 7 \times 10^{19}$ atoms). However, the AD sample having 2 times larger mass, the maximal number of accessible He atoms per one C atom was 3% in the LV sample and 1.5% in the AD sample; this fact together with the different sample topologies (characterized with N_t) are crucial in our interpretation of C_{ads}.

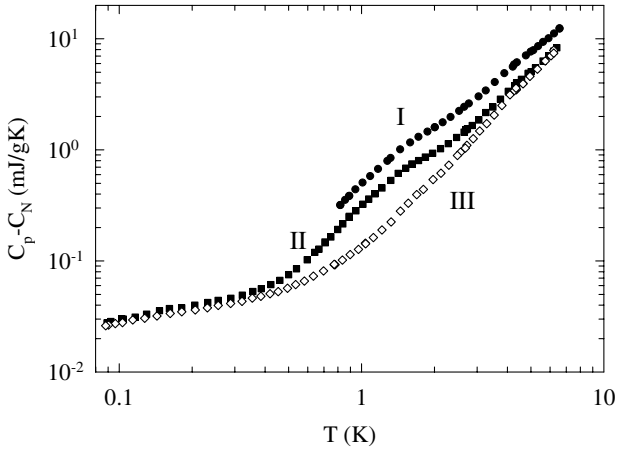

FIG. 1. Vibrational specific heat $C_{\text{vib}} = C_p - C_N$ of the AD sample (per g of sample): pristine state (without He)—III; intermediate adsorption—II; maximum adsorption in our experimental conditions (see text)—I.

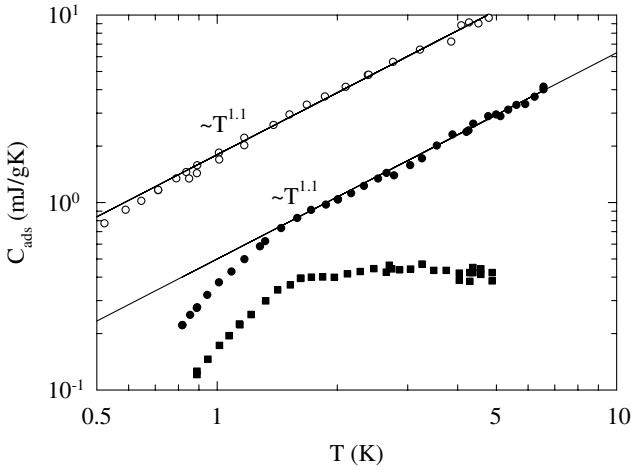

FIG. 2. Specific heat of He^4 adsorbate (after subtraction of the corresponding pristine values; C_{ads} *per g of sample*), for LV and AD sample. Data (○) and (●) are for maximum adsorption for the LV sample (3 at.% of C atoms) and the AD sample (1.5 at.%), respectively. Data (■) correspond to the AD sample at intermediate adsorption.

C_{ads} represents at least 50% of the total C_p (at 1 K) in our conditions. It exhibits a *striking similarity* for both samples which certainly reflects the same thermodynamics of the additional contribution coming from the adsorbed He. Figure 2 shows that in the case of maximum adsorption both samples follow a close to linear-in-T behavior, with a smooth crossover to a stronger T dependence below 1 K. If we take into account that the number of available He atoms per one C atom is 2 times larger for the LV sample, the relative amplitude of C_{ads} of LV is still almost 2 times larger than for the AD sample.

For the intermediate adsorption state there is again a similar qualitative behavior for both systems (initial rise and a saturation: inset of Fig. 3), but the rising part in the log plot reveals very specific differences. Figure 3 demonstrates, very likely for the first time, the prototype behavior of the 2D Debye model (T^2 rise) and the 1D Einstein model (exponential rise), in the experimental data of C_p in the same physical system. Only the T^2 (2D) behavior has been determined in He films [4–6]. However, the *plateau value of* C_{ads} *per He atom* should also indicate the effective dimensionality for the He atomic excitations, being 0.5 k_B for 1D gas or 1 k_B for a 2D fluid (gas or liquid), found also in recent theoretical models on the gas confined in NTs [16,17]. The plateau values surpassing 1 k_B would mean the occupation of excited single-particle states in the perpendicular direction, announcing the 3D ordering.

In order to estimate the corresponding number of He adatoms in the partially outgassed states (Fig. 3), we have used information from the desorption experiments performed in quite similar conditions as here [12,18]. Although they show some disagreement in the absolute values, there is rather good agreement for the ratios of the adsorbed He between two desorption temperatures (T_D). For our outgassing conditions, $T_D \sim 15$ K for AD and $T_D \sim 25$–30 K for the LV sample, the ratio should be $N_{AD}/N_{LV} = 2$. We estimate also $N_{AD} \sim N_0/10$ (normalizing with N_0, sample mass and T_D in Ref. [12]) and finally we get $N_{AD} \sim 7 \times 10^{18}$ and $N_{LV} \sim 3.5 \times 10^{18}$. Here, we note that even very accurately measured total He density, as in the case of He films [see Refs. [4,6]], can be misleading in the interpretation of results, especially at so low coverages, due to the surface heterogeneity. The absolute values of C_{ads} (Fig. 3 inset) —0.038 mJ/K for AD (90 mg) and 0.045 mJ/K for the LV (45 mg) sample — yield corresponding plateau values per one He atom — 0.4 k_B for AD and 0.95–1.0 k_B for LV, consistent with the theoretical expectations.

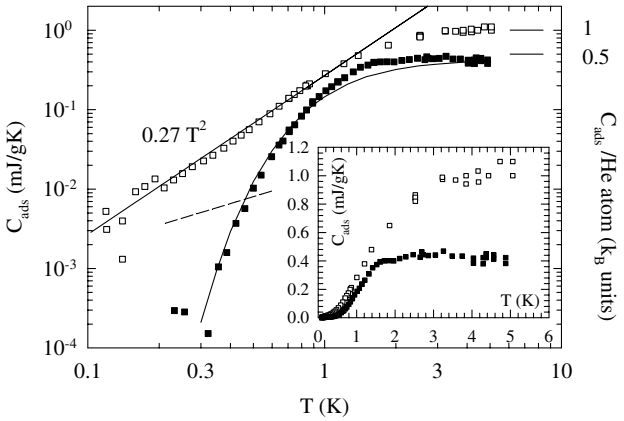

FIG. 3. Specific heat of the He^4 adsorbate at intermediate adsorption: (□) state A of the LV sample and (■) state II of the AD sample. Data (■) below 1 K are fitted by an Einstein specific heat, with $\Theta_E = 3.8$ K, and data (□) by a quadratic variation below 1.5 K. The same data are plotted in a linear plot in the inset. The plateau values recalculated per atom of He correspond to 1 k_B for LV and 0.4 k_B for AD sample. The dashed line is the residual term which was removed in the case of the AD sample [14].

It is very difficult to reconcile these extreme cases (2D-LV behavior and 1D-AD behavior) if one considers only the *absolute number* of He adatoms, $N_{AD} > N_{LV}$, which seems to lead to the inverse effect. In fact, contrary to the case of He films on planar substrates where the He behavior is surprisingly independent of the structure of the substrate [5], here we are in the case where the *topology of the substrate plays an essential role.* This appears to be a natural conclusion in the case of C-nanotube bundles. That finally gives the opportunity to detect 1D effects in confined He (in a very diluted limit), which was not possible (or evidenced) in low-T He films.

The essential topological difference between AD and LV samples is the main *size of the bundles* [7,8]. We neglect the certain distribution in size supposing that AD bundles have 19 tubes and LV 61 (corresponding to three or five tubes on each facet in regular hexagonal arrays). There are three specific sites of adsorption for He [19]: interstitial channels (IC), outer grooves, (G) and bundle surface (S). Recent adsorption isotherm measurements [20], consistent with He desorption experiments [12,18], indicate that adsorption is first in the outer grooves of the bundles, then filling the rest of the outer surface, and finally layering on the outer surface (in successive layers). Monte Carlo simulations [21] show an extremely pressure-sensitive crossover from 2D coverages to 1D filling, which successively leaves G and finally IC as the last refuge for the He atoms.

From N_{AD} and N_{LV}, we now try to find the possible occupied places, either in outer 2D graphene surfaces or 1D (IC and G) channels using these topological considerations. We start from an effective adsorption surface of $\sim$300 m^2/g per nanotube, in good correspondence with 80 m^2/g for a typical bundle of $N_t = 37$ [20]. A complete coverage of external surfaces (2D sites) varies between 12 and 9 He sites (between two grooves on facets) for AD and LV ($N_t = 19$ and 61, respectively). Taking also in account the possible adsorption in the 1D channels (G + IC), this yields $S_{eff} = 100$ m^2/g for $N_t = 19$, and 70 m^2/g for $N_t = 61$, with 80% and 66% of sites in surface, respectively. For our sample masses, we get

2.0 m^2 of effective surfaces for 1D channels and 7.0 m^2 for the external surface in the AD sample, and 1 m^2 for 1D and 2.0 m^2 for the surface of the LV sample. We suppose that adsorption takes place in the same external conditions (i.e., supposing similar binding potentials) and that 12 atoms/nm^2 is a complete layer coverage, as for He films. Consequently, the final configurations for the total desorption of N_0 atoms of He at $T = 4$ K should be for the AD sample: all 1D channels occupied and around 1/2 of the outer surface of bundles and for the LV sample: all 1D channels, two external layers occupied, and 50% of a third layer.

Outgassing starts from the outer surfaces and continues with atoms at the lower surfaces. In the case of the AD sample ($T_D = 15$ K and remaining $N_{\mathrm{AD}} \sim 7 \times 10^{18}$), first all He atoms of the surface ($\sim 5 \times 10^{19}$) were degassed [19,21]. Further degassing empties the groove regions [16] and probably also some weakly bond IC sites (in total 0.7×10^{19}) [21]. Finally, He remains only in some IC sites [16,21]; i.e., about 50% of the IC sites are still occupied. This is the origin of 1D He confinement behavior in AD as demonstrated in Fig. 3. Also consistent with our 1D interpretation for the AD sample is the very rapid decrease of the He heat capacity below 1 K, which can be well fitted with an Einstein function, varying like $(\Theta_E/T)^2 \exp(-\Theta_E/T)$, with $\Theta_E = 3.8$ K (Fig. 3). This indicates independent harmonic oscillators, probably localized. To our knowledge, the exponential decay has never been observed in He^4 on grafoil. It was supposed to occur at very low coverage, i.e., with a very feeble C_p signal [4,5].

For the LV sample, outgassing is of a higher cost in energy because one has to outgas the successive layers and the corresponding desorption energy should be much larger for completely removing the first layer [20]. The heat of adsorption of the second layer for He on grafoil is very large (35 K) in comparison to the third (15 K) and the following [4]. We conclude that, even at a desorption temperature of 25–30 K, there remains still a considerable number of 2D He coverages for this sample. This is consistent with the 2D behavior of C_{ads}, which clearly shows a quadratic regime over more than one decade in T; $C_{\mathrm{ads}} = 0.27$–$0.28\ T^2$ (mJ/g K) (Fig. 3). This is the signature of a 2D — fluid or solid — regime for adsorbed He. For the fluid case, consistent with the limit $C/R \rightarrow 1$ (R is the gas constant), for the molar heat capacity of He, the corresponding 2D Debye temperature for only longitudinal phonons is $C_{\mathrm{ph}} = 14.42R(T/\theta)^2$ [22], so that $C_{\mathrm{ads}} = 2.1\ T^2$ (J/mol K) yields $\theta = 7.5$ K. This value can be compared to 5.1 K obtained in the same T range (0.1–0.5 K) for the first layer of He^4 on grafoil [4]. In addition, the amplitude of the T^2 regime (or the Debye T) is rather independent of the order of the layer up to the third one [4(a)].

In conclusion, we gave the first thermodynamical evidence of 1D confinement of He in NT bundles, as well as 2D behavior of C_{ads} for bundles with a larger size. These results suggest further studies of the crossover between 1D to 2D adsorbate behavior by varying, for a given topology of the NT bundles, the concentration of He atoms in the dilute limit. This is of great significance, since it may give basic information on the very low energy states of He (zero-point energy, localization, etc.). The remarkable absence of peaks of C_{ads} in this T range indicates a strong influence of size effects imposed by NT bundles compared to conventional He films, such as on grafoil. This could be accounted for by a much shorter correlation length which inhibits the development of structural phase transitions. One result which remains to be explained is $C_{\mathrm{ads}} \sim T^{1.1}$ for rather large adsorption levels (a few at.%) of He, when the adsorbate behavior is essentially determined by the external "dressing" of the bundles. This seems to be a completely new physics in comparison to the previous results obtained for the successive layering processes on purely 2D substrates like grafoil and deserves some theoretical consideration.

A. Šiber, L. Firlej, B. Kuchta, and H. Godfrin are grately acknowledged for stimulating discussions and D. Starešinić for his help.

[1] J. Hone *et al.*, Science **289**, 1730 (2000).
[2] M. V. Cole *et al.*, Phys. Rev. Lett. **84**, 3883 (2000).
[3] J. C. Lasjaunias *et al.*, Phys. Rev. B **65**, 113409 (2002).
[4] (a) D. S. Greywall and P. A. Busch, Phys. Rev. Lett. **67**, 3535 (1991); (b) D. S. Greywall, Phys. Rev. B **47**, 309 (1993).
[5] R. L. Elgin and D. L. Goodstein, Phys. Rev. A **9**, 2657 (1974).
[6] M. Bretz *et al.*, Phys. Rev. A **8**, 1589 (1973).
[7] S. Rols *et al.*, Eur. Phys. J. B **10**, 263 (1999).
[8] J. L. Sauvajol and R. Almairac (private communication).
[9] A. Thess *et al.*, Science **273**, 483 (1996).
[10] C. Journet *et al.*, Nature (London) **388**, 756 (1997).
[11] N. Bendiab *et al.*, J. Appl. Phys. **93**, 1769 (2003).
[12] W. Teizer *et al.*, Phys. Rev. Lett. **82**, 5305 (1999); **84**, 1844(E) (2000).
[13] $C_N = 0.15\ T^{-2}$ (μJ/g K) found for AD is 25 times smaller in amplitude than for LV [3].
[14] A slight variation (7%) of the power law $T^{0.34}$ contribution between runs II and III of the AD sample (see Fig. 1) was analyzed as $0.015\ T^{0.9}$ (mJ/g K) (dashed line in Fig. 3) and subtracted in order to obtain the residual C_{ads} (due only to adsorbed He).
[15] J. C. Lasjaunias *et al.*, Nanotechnology (to be published).
[16] A. Šiber, Phys. Rev. B **66**, 205406 (2002), and references therein.
[17] M. M. Calbi *et al.*, Rev. Mod. Phys. **73**, 857 (2001).
[18] Y. H. Kahng *et al.*, J. Low Temp. Phys. **126**, 223 (2002).
[19] G. Stan *et al.*, Phys. Rev. B **62**, 2173 (2000).
[20] T. Wilson and O. E. Vilchies, Physica (Amsterdam) **329B**, 278 (2003).
[21] L. Firlej and B. Kuchta (to be published).
[22] J. G. Dash, J. Low Temp. Phys. **1**, 173 (1969)